JETS, $W^{\pm}$ AND Z^0 PRODUCTION IN UA2*

THE UA2 COLLABORATION
BERN–CERN–COPENHAGEN (NBI)–HEIDELBERG–ORSAY (LAL)–
PAVIA–PERUGIA–PISA–SACLAY (CEN)

PRESENTED BY HANS HÄNNI

CERN, Geneva, Switzerland

(Received February 3, 1986)

We present new results on the production of hadron jets and of Intermediate Vector Bosons at the CERN $\bar{p}p$ Collider at $\sqrt{s} = 630$ GeV. Comparisons are made with data previously collected at $\sqrt{s} = 546$ GeV, and with theoretical predictions from QCD and the Standard Model of the electroweak interaction.

PACS numbers: 13.85.–t

1. Introduction

The UA2 collaboration has already reported experimental results on the production of jets [1] and of the Intermediate Vector Bosons $W^{\pm}$ and Z^0 [2]. The data were collected at the CERN SPS $\bar{p}p$ Collider in the period 1981–1983 at $\sqrt{s} = 546$ GeV, for a total integrated luminosity $\mathscr{L} = 142\,\text{nb}^{-1}$. In the subsequent run during Autumn 1984 the Collider operated at an increased energy, $\sqrt{s} = 630$ GeV, and the total luminosity accumulated by the UA2 experiment was $\mathscr{L} = 310\,\text{nb}^{-1}$. The analyses presented here refer to both data samples, which are combined only for the determination of the intrinsic W and Z^0 parameters. The UA2 experimental apparatus [3] is essentially a highly segmented, tower structured calorimeter with complete cylindrical symmetry in azimuth and full coverage in the polar range ($20° < \theta < 160°$). In addition it provides for charged particle momentum measurement in the regions ($20^0 < \theta < 40°$; $140° < \theta < 160°$), where only electromagnetic calorimetry is present. Fig. 1 shows a schematic view of the longitudinal cross section of the detector in a plane containing the beam axis. In this apparatus electrons are measured with an energy resolution $\Delta E \approx 0.15\sqrt{E}$ (E in GeV), with a systematic uncertainty of $\approx \pm 1.5\%$; the energy resolution for jets is $\Delta E^j/E^j \approx 0.32\ (E^j)^{-0.25}$ (E^j in GeV).

* Presented at the XXV Cracow School of Theoretical Physics, Zakopane, Poland, June 2–14, 1985.

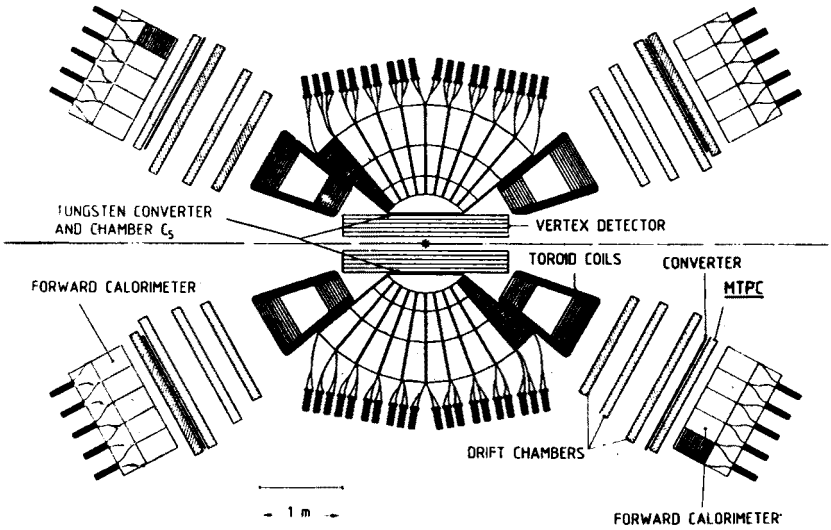

Fig. 1. Longitudinal cross section of the UA2 detector in a plane containing the beam axis

2. *Inclusive jet production*

After rejecting a small background contamination, a clustering algorithm applied to the transverse-energy pattern of the calorimeter cells yields the transverse energy of hadronic jets. Jet directions are determined from the position of the weighted cluster centroids with respect to the center of the interaction region. The inclusive differential cross sections for jet production at $\eta = 0$ are shown in Fig. 2a as a function of jet transverse momentum p_T for both Collider energies. An overall systematic uncertainty of $\pm 45\%$ applies to the data.

The results are well described by a QCD calculation, shown by the curves in Fig. 2, which assumes $Q^2 = p_T^2$, $\Lambda = 200$ MeV and the structure functions by Eichten et al. [4]. The ratio of the two cross sections, displayed in Fig. 2b, is a rising function of transverse momentum and is also well described by the calculation. Similar results are obtained for the invariant-mass distribution of inclusive jet-pair production, with both jets within $|\eta| < 0.85$.

Possible deviations of these data from the QCD predictions at high values of p_T can be parametrized in terms of a new energy scale Λ_c, representing through a contact term the effective energy scale of a new interaction at the preon level [5]. The data require values of $\Lambda_c > 370$ GeV at the 95% confidence level (Fig. 2a).

3. $W^{\pm}$ *production cross section and mass*

Fig. 3a shows the distribution of the transverse momentum p_T^e for all electrons above 11 GeV/c identified in the standard UA2 analysis [2]. A significant population with $p_T^e \geqslant 25$ GeV/c is evident, as expected from $W^{\pm}$ decay. Other contributions include Z^0

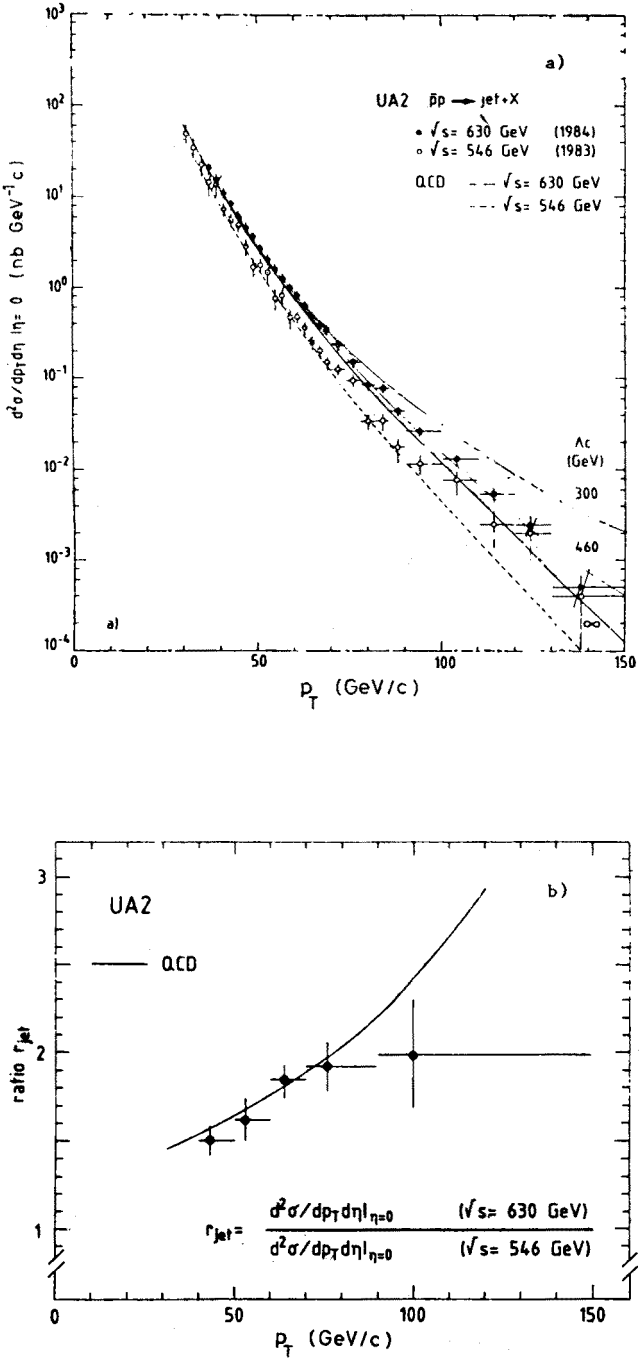

Fig. 2. a) Inclusive jet production cross sections at $\sqrt{s}$ = 546 GeV and 630 GeV. The curves are a QCD calculation (see text). b) Comparison of the ratio of inclusive jet cross sections with a QCD calculation (see text)

decays, electrons from semileptonic decay of heavy quarks, electrons from the τ decay mode of $W^{\pm}$, and a contribution of jets misidentified as electrons.

To extract from the data the $W^{\pm}$ signal we apply a topological cut using the quantity

$$\varrho_{\mathrm{opp}} = -\vec{p}_{\mathrm{T}}^{\,\mathrm{e}} \cdot \sum \vec{p}_{\mathrm{T}}^{\,\mathrm{jet}} / |\vec{p}_{\mathrm{T}}^{\,\mathrm{e}}|^2,$$

where the sum extends to all energy clusters having an azimuthal separation $\Delta\phi > 120°$ to the electron candidate and $p_{\mathrm{T}} > 3$ GeV/c. The sample is then split into two categories:

a) Events with $\varrho_{\mathrm{opp}} < 0.2$: this sample contains events which are unbalanced in p_{T}, and therefore include most $W \to e\nu$ candidates.

b) Events with $\varrho_{\mathrm{opp}} \geqslant 0.2$: this sample contains mostly balanced events, among which $Z^0 \to e^+e^-$. It is dominated by two-jet background with one jet misidentified as an electron and it is used to estimate the background to the W sample.

The $p_{\mathrm{T}}^{\mathrm{e}}$ distribution of the 592 events satisfying $\varrho_{\mathrm{opp}} < 0.2$ is shown in Fig. 3b. The background from QCD processes is superimposed (.....), together with expected contributions from decays $W \to \tau\nu$ (.....) and $Z^0 \to e^+e^-$ with one electron escaping the detector acceptance (------). The expected contribution of $W \to e\nu$ decays (.....) is shown, together with the expected total from all processes. For $p_{\mathrm{T}}^{\mathrm{e}} > 25$ GeV/c the histogram contains 119 events, with a background of 5.8 ± 1.7 events.

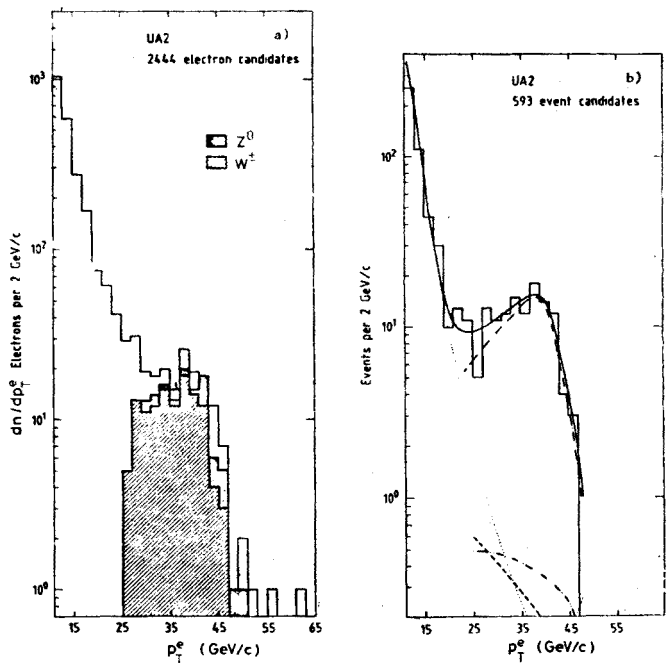

Fig. 3. a) The electron p_{T} spectrum of all UA2 data. b) 593 events satisfying $p_{\mathrm{T}}^{\mathrm{e}} > 11$ GeV/c and $\varrho_{\mathrm{opp}} < 0.2$. The expected background from QCD processes is superimposed (·····) together with expected contributions from decays $W \to \tau\nu$ (– – – –) and $Z^0 \to e^+e^-$ with one electron escaping the acceptance (··–··–··). The contribution of $W \to e\nu$ decays is shown (·–·–·–), together with the total expectation from all processes (———)

A value of the W mass can be obtained from the electron candidates with $\varrho_{opp} < 0.2$ using two different methods:

1. The p_T^e distribution of Fig. 3b is compared with that expected from $W \to e\nu$ decay. A Monte Carlo program is used to generate the electron differential distribution p_T^e for different values of the W mass, taking into account the detector response and using structure functions from Glück et al. [6], the W transverse momentum distribution from Altarelli et al. [7] and a fixed W width, $\Gamma_W = 2.7\ \mathrm{GeV}/c^2$. A maximum likelihood fit to the data gives a value $M_W = 80.6 \pm 1.1\ \mathrm{GeV}/c^2$, where the quoted error is only statistical; an additional systematic error of $\approx 1\ \mathrm{GeV}/c^2$ results from the uncertainty on the assumptions used to generate the Monte Carlo distributions.

2. The transverse mass distribution of the event sample (Fig. 4) is compared with distributions generated by Monte Carlo for various values of M_W. We find that the transverse mass distribution depends only weakly on p_T^W and suffers no distortions from the ϱ_{opp} cut. The best fit value of M_W obtained by this method is $M_W = 81.2 \pm 1.0\ \mathrm{GeV}/c^2$, with an additional systematic error of $\pm 0.5\ \mathrm{GeV}/c^2$.

Although the two methods give consistent results, we prefer to quote the mass value obtained by the latter method because of the smaller systematic error, which we add in quadrature to the statistical error. To summarize we quote

$$M_W = 81.2 \pm 1.1\ (\mathrm{stat.}) \pm 1.3\ (\mathrm{syst.})\ \mathrm{GeV}/c^2,$$

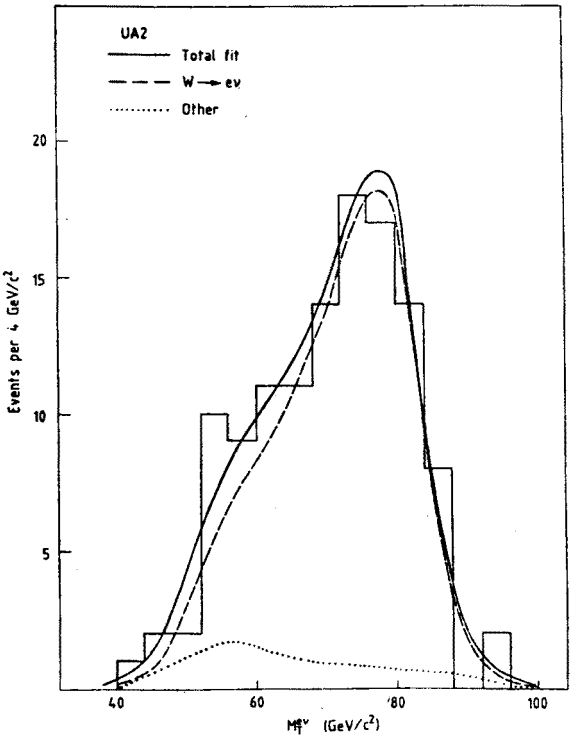

Fig. 4. Transverse mass distribution for events with $p_T^e > 17\ \mathrm{GeV}/c$, $p_T^\nu > 25\ \mathrm{GeV}/c$

where the systematic error is due to a $\pm 1.6\%$ uncertainty on the calorimeter calibrations. For the width of the W, we quote an upper limit $\Gamma_W < 7$ GeV/c^2 at the 90% confidence level.

The main effects of non-leading corrections to W production are to increase the production cross section by a factor $\sim 30\%$ and to give the W a sizeable average transverse momentum p_T^W [7]. For relatively large values of p_T^W, the W bosons are expected to recoil against hadronic jets. To study these effects we cannot use the sample which satisfies the

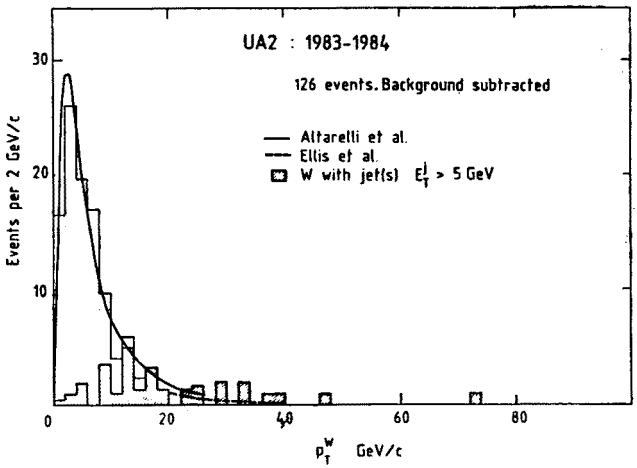

Fig. 5. Distribution of p_T^W for 126 events (less 9.8 background) from the 1983–84 data sample, satisfying $p_T^e > 15$ GeV/c and $p_T^\nu > 25$ GeV/c. The shaded region corresponds to 36 events having at least one jet of $E_T^j > 5$ GeV. The superimposed full curve is from Altarelli et al. [7], using D01 structure functions and calculated at $\sqrt{s} = 630$ GeV. The dotted curve is from Ellis et al. [21] at $\sqrt{s} = 630$ GeV

requirement $\varrho_{opp} < 0.2$, because this cut rejects electrons in the presence of jets at opposite azimuthal angles. We use instead a sample of events containing an electron candidate with $p_T^e > 15$ GeV/c and having at the same time a missing transverse momentum in excess of 25 GeV/c. This sample contains 126 events with a background estimate of 10.8 events. The distribution of W transverse momentum is shown in Fig. 5 together with a QCD prediction by Altarelli et al., [7] in good agreement with the data. The average value of p_T^W is 8.8 GeV/c, with a systematic uncertainty of about 2 GeV/c.

The cross section for $W^\pm$ production followed by the decay $W \to e\nu$ is measured to be:

$$\sigma_W^e = 0.50 \pm 0.09\,(\text{stat.}) \pm 0.05\,(\text{syst.})\ \text{nb}, \quad \sqrt{s} = 546\ \text{GeV},$$

$$\sigma_W^e = 0.53 \pm 0.06\,(\text{stat.}) \pm 0.05\,(\text{syst.})\ \text{nb}, \quad \sqrt{s} = 630\ \text{GeV},$$

The corresponding theoretical predictions [7] are $\sigma_W^e = 360^{+110}_{-50}$ and $\sigma_W^e = 450^{+140}_{-80}$ pb, where the errors reflect theoretical uncertainties. The increase of the W production cross section between the two $\sqrt{s}$ values is measured to be

$$r = \sigma_W^e(\sqrt{s} = 630)/\sigma_W^e(\sqrt{s} = 546) = 1.06 \pm 0.23$$

in good agreement with the theoretical prediction $r = 1.27$.

4. Charge asymmetry

At the energies of the CERN $\bar{p}p$ Collider, W production is dominated by $q\bar{q}'$ annihilation involving at least one valence quark (antiquark). As a consequence of V−A coupling, the W is produced with almost full polarisation along the direction of the incident $\bar{p}$ beam, and a distinctive charge asymmetry can be observed in the decay $W \to e\nu$.

If θ^* is the angle between the charged lepton and the direction of the incident proton in the W rest frame, the angular distribution has the form

$$dn/d(\cos\theta^*) \propto (1-q\cos\theta^*)^2+2q\alpha\cos\theta^*, \tag{1}$$

where $q = -1$ for electrons and $+1$ for positrons. The parameter α, with the property $0 \leqslant \alpha \leqslant 2$, depends on the ratio x between the A and V couplings (time reversal invariance requires x to be real). Under the assumption that x is the same for both Wqq and Wev couplings, α is given by

$$\alpha = [(1-x^2)/(1+x^2)]^2. \tag{2}$$

For standard V−A coupling α is zero. We note that the angular distribution given by Eq. (1) provides no information on either the relative sign or the relative strength (i.e. the choice of x or $1/x$) of the V and A coupling.

In the UA2 detector a determination of the charge sign is only possible in the forward detectors, where a magnetic field is present. Since the sensitivity of the data to the exact form of the angular distribution is highest for values of $\cos\theta^*$ close to ± 1, corresponding to small values of p_T^e, we consider all electron candidates with $p_T^e > 20$ GeV/c and $\varrho_{opp} < 0.2$ that are detected in the forward regions.

This sample contains 28 events with an estimated background of 2 events. A comparison between the electron momentum p and the energy E, as measured in the calorimeter, is made in Fig. 6. This figure shows the position of these events in the plane (p^{-1}, E^{-1}), where p is the momentum with the sign of $q\cos\theta_e$ (θ_e being the laboratory angle of the electron with respect to the proton direction). The horizontal error bars in Fig. 6 represent the uncertainty on the measurement of p^{-1}, which is 0.007 $(\text{GeV}/c)^{-1}$. There are 20 events in the region of negative p values (the region favoured by the V−A coupling), and 8 events in the region of positive p values, corresponding to an asymmetry of 0.43 ± 0.17. This value is in good agreement with the expected asymmetry for V−A coupling of 0.53 ± 0.06 ($\alpha = 0$ in Eq. (1)), as obtained by a Monte Carlo calculation which takes into account the expected sea-quark contribution, and as well a background contribution which is estimated to include 0.6 events from $Z^0 \to e^+e^-$ decay with one of the two electrons undetected and 0.3 events resulting from $W \to \tau\nu$ decay.

To extract a value of α from these data we use a Monte Carlo program to compare the expected two-dimensional distributions $f^{\pm}(p_T^e, \theta_e)$, for positrons and electrons separately, with those observed. To each event we assign a likelihood $Q_i = f^+\eta^+ + f^-\eta^-$, where $\eta^+(\eta^-)$ is the probability that the observed particle was a positron (an electron). The functions $f^{\pm}$ take into account the W motion, and the probabilities $\eta^{\pm}$ include the uncertainty of the charge measurement resulting from the momentum measurement error.

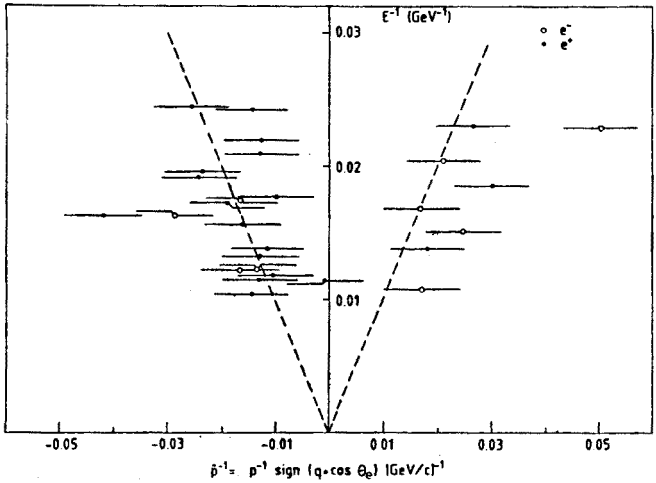

Fig. 6. Plot of $\hat{p}^{-1}$ vs. E^{-1} for 28 W $\rightarrow$ ev candidates with $p_T^e > 20$ GeV detected in the forward regions. The quantity $\hat{p}$ is the product of the electron momentum (as measured by magnetic deflection) and the sign of the product $q \cdot \cos\theta_e$, where $q = +1(-1)$ for $e^+(e^-)$. θ_e is the electron angle with respect to the proton direction

After taking account of biases of the maximum-likelihood estimator, we measure α to be consistent with zero, as expected for V−A coupling. We determine $\alpha < 0.39$ (68% confidence level), corresponding to $0.48 < |x| < 2.1$ (see Eq. (2)).

5. Z^0 production and decay

A first selection of events on the 1984 data sample, requiring only two electromagnetic clusters in the calorimeter with invariant mass M_{ee} above 20 GeV/c^2, leaves a total of 1154 events. Their mass distribution is shown in Fig. 7a. A clear accumulation is already visible in the Z^0 region. The additional requirement that at least one cluster satisfies all electron identification criteria [2] selects 54 events, whose mass distribution is shown in Fig. 7b. There is a clear peak in this distribution, consisting of 8 events with a mass value in excess of 75 GeV/c^2, with a background contamination of 0.21 ± 0.02 events. Fig. 8 shows the mass values and the measurement errors for the total Z^0 sample of UA2; we note that the mass values of the 1982–1983 events were slightly readjusted following a recalibration of the calorimeter response. A fit to the Z^0 mass yields:

$$M_Z = 92.5 \pm 1.3\,(\text{stat.}) \pm 1.5\,(\text{syst.})\ \text{GeV}/c^2,$$

where the systematic error reflects the $\pm 1.6\%$ uncertainty on the absolute energy scale of the calorimeter.

The cross section for Z^0 production followed by $Z^0 \rightarrow e^+e^-$ is measured to be:

$$\sigma_Z^e = 110 \pm 39\,(\text{stat.}) \pm 9\,(\text{syst.})\ \text{pb}, \quad \sqrt{s} = 540\ \text{GeV},$$

$$\sigma_Z^e = 52 \pm 19\,(\text{stat.}) \pm 4\,(\text{syst.})\ \text{pb}, \quad \sqrt{s} = 630\ \text{GeV}.$$

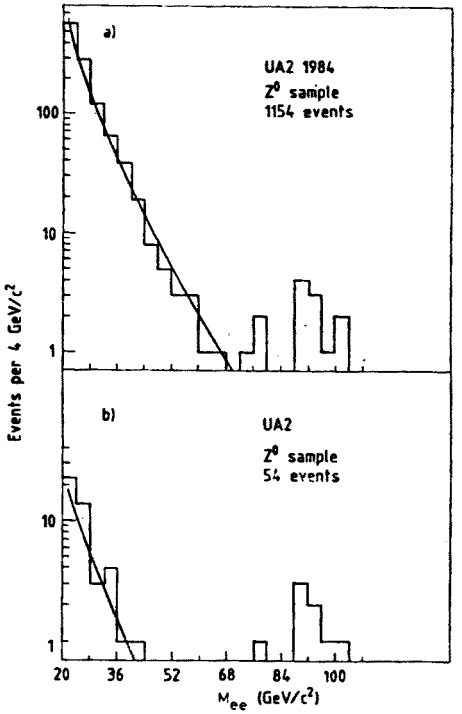

Fig. 7

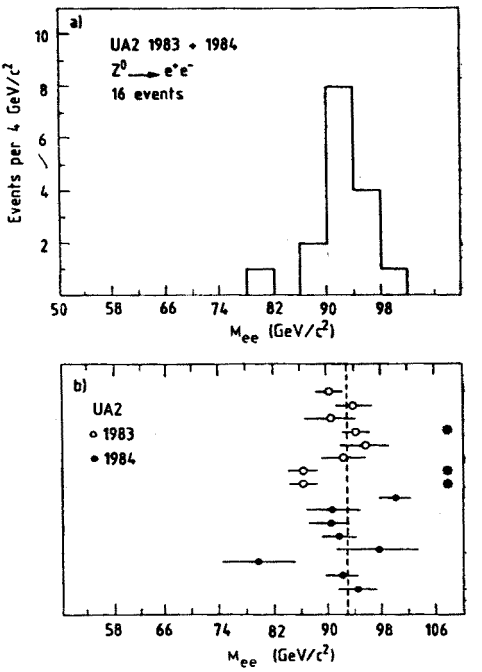

Fig. 8

Fig. 7. Electron pair mass spectrum from the 1984 data, a) after calorimeters cuts on both electron candidates, b) after requiring that at least one of the two candidates be a certified electron

Fig. 8. a) The Z^0 mass peak of the entire UA2 sample. b) Mass values and errors of the individual Z^0 candidates. Those marked (*) are not used in the mass determination because of systematic uncertainties of the measurement

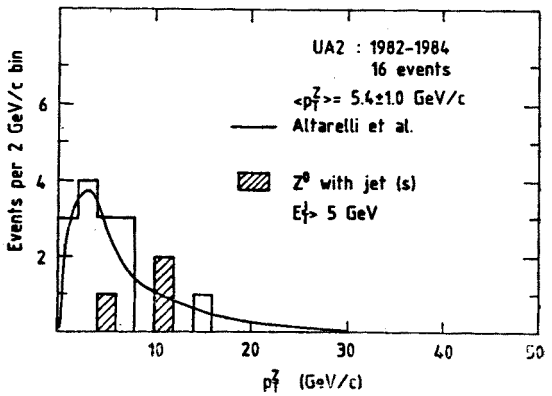

Fig. 9. The Z^0 transverse momentum distribution

Both values are consistent with theoretical predictions [7], which give $\sigma_Z^e = 42^{+13}_{-6}$ pb and 51^{+16}_{-10} pb at $\sqrt{s} = 540$ and 630 GeV, respectively.

Fig. 9 shows the distribution of the Z^0 transverse momentum, p_T^Z, for all 16 events, together with the result of a QCD calculation [7]. The average value of p_T^Z is 5.4 ± 1.0 GeV/c.

6. *The width of the Z^0*

In order to extract an estimate of the Z^0 width, Γ_Z, from the 13 events used to determine M_Z, we first note that the r.m.s. deviation of the mass values from the value of M_Z given by Eq. (12) is 3.58 GeV/c^2, which is very similar to the average of the measurement errors, $\sigma = 3.42$ GeV/c^2. Under these circumstances, and given the small statistical sample available, the determination of Γ_Z depends critically on a precise knowledge of the experimental mass resolution function. For this reason we prefer to quote an upper limit to Γ_Z, which we obtain by using a Monte Carlo program to generate a large number of event samples, each consisting of 13 $Z^0 \to e^+e^-$ events, according to a Breit-Wigner shape and taking into account the detector resolution. We have investigated several estimators to take account of the biases introduced by the small statistical sample. Using an estimator ω which minimizes the bias due to low statistics, we measure $\Gamma_Z < 3.3$ GeV/c^2 at the 90% confidence level, from the Γ_Z value for which $\omega < \omega_{exp}$ in 10% of the Monte Carlo event samples (ω_{exp} is the value of the estimator for the real event sample). Using the maximum-likelihood estimator, which is biased, we measure $\Gamma_Z < 4.6$ GeV/c^2 at the 90% confidence level.

Within the context of the Standard Model, the value of Γ_Z is related to the number of fermion doublets for which the decay $Z^0 < f\bar{f}$ is kinematically allowed. In the case for which any additional W and Z^0-decay products result from new fermion doublets in which only the neutrino is significantly less massive than $M_Z/2$, then:

$$\Gamma_Z(\text{meas}) = \Gamma_Z(\text{three fermion families}) + 0.177\, \Delta n_\nu, \tag{3}$$

where Γ_Z is in units of GeV/c^2, and Δn_ν is the number of additional neutrino species.

Since Γ_W is independent of Δn_ν in this context, if the associated charged lepton mass is large, an independent estimate of Γ_Z can be obtained by measuring the ratio $R = \sigma_Z^e/\sigma_W^e$. In this case the error on R is dominated by statistics, because the value of the total integrated luminosity cancels out. From the observed numbers of $W \to e\nu$ and $Z^0 \to e^+e^-$ decays, and the corresponding detection efficiencies, we measure $R = 0.136^{+0.041}_{-0.033}$, averaged over the data of $\sqrt{s} = 546$ GeV and $\sqrt{s} = 630$ GeV. QCD estimates of the ratio between the Z^0 and W production cross-sections [7] provide a relationship between R and the ratio Γ_W/Γ_Z:

$$\Gamma_W/\Gamma_Z = (8.9 \pm 0.9)R, \tag{4}$$

where the error reflects the uncertainty of the QCD calculation [7] as well as the uncertainties of the values used for the partial widths. To calculate the partial widths we have used the measured M_W and M_Z values together with their errors.

Using the Standard Model value, $\Gamma_W = 2.65\ \mathrm{GeV}/c^2$ (which corresponds to the measured mass $M_W = 81.2\ \mathrm{GeV}/c^2$ and to a t-quark mass $m_t = 40\ \mathrm{GeV}/c^2$), we find

$$\Gamma_Z = 2.19^{+0.70}_{-0.50}\,(\mathrm{stat.}) \pm 0.22\,(\mathrm{syst.})\ \mathrm{GeV}/c^2 \tag{5}$$

in good agreement with the Standard Model prediction of $\Gamma_Z = 2.72\ \mathrm{GeV}/c^2$ for $M_Z = 92.5\ \mathrm{GeV}/c^2$, assuming three fermion families and $m_t = 40\ \mathrm{GeV}/c^2$. We evaluate an upper limit for Δn_ν at the 90% confidence level from the lower limit $R > 0.094$, which gives $\Gamma_Z < 3.17 \pm 0.31\ \mathrm{GeV}/c^2$. We obtain $\Delta n_\nu < 2.6 \pm 1.7$ (the errors reflect the uncertainties of Eq. (4)).

The quoted limit on the additional number of neutrinos is valid subject to very specific conditions noted above. In most models for which an increase in Γ_Z is expected (for example the decay of Z^0 into super-symmetric particles) the Standard Model prediction for Γ_W is also affected.

7. Comparison with the SU(2) ⊗ U(1) model

If we ignore the fermion and Higgs scalar masses, and the elements of the Kobayashi-Maskawa matrix [8], the minimal Standard Model is characterised by three parameters, which can be taken to be α (the fine structure constant), and the IVB masses M_W, M_Z. In order to compare our measurements with the predictions of the Standard Model, we must use suitably renormalised and radiatively corrected theoretical quantities [9]. We shall use the scheme where [10]

$$\sin^2\theta_W = 1 - (M_W/M_Z)^2 \tag{6}$$

which leads to the following predictions for the IVB masses:

$$M_W^2 = A^2/[(1-\Delta r)\sin^2\theta_W], \tag{7}$$

$$M_Z^2 = 4A^2/[(1-\Delta r)\sin^2 2\theta_W], \tag{7'}$$

where $A = (\pi\alpha/\sqrt{2}G_F)^{1/2} = (37.2810 \pm 0.0003)\ \mathrm{GeV}/c^2$ using the measured values of α and G_F [11]. In the above equations, the value Δr reflects the effect of one-loop radiative corrections on the IVB masses and has been computed to be [10]

$$\Delta r = 0.0696 \pm 0.0020 \tag{8}$$

for $m_t = 36\ \mathrm{GeV}/c^2$ and assuming that the mass of the Higgs boson, M_H, is equal to M_Z. Although that quoted theoretical error in Eq. (8) is quite small, it has been pointed out [10, 12] that Δr can be significantly decreased in the case of a very heavy t-quark ($\Delta r \approx 0$ for $m_t = 240\ \mathrm{GeV}/c^2$), or if a new fermion family exists with a large mass splitting between the two members of an SU(2) doublet.

Using Eqs (7), (7') and (8), we can extract two values of $\sin^2\theta_W$ from our measured values of M_W and M_Z. We then combine them to obtain our best estimate of $\sin^2\theta_W$:

$$\sin^2\theta_W = 0.226 \pm 0.005\,(\mathrm{stat.}) \pm 0.008\,(\mathrm{syst.}). \tag{9}$$

By using Eq. (6) it is possible to measure $\sin^2\theta_W$ with no systematic error from the uncertainty on the mass scale. We recall, however, that there is a ± 0.5 GeV/c^2 systematic uncertainty on the value of M_W which is not related to the energy calibration of the calorimeter (see Section 7). By taking this uncertainty into account we obtain

$$\sin^2\theta_W = 0.229 \pm 0.030\,(\text{stat.}) \pm 0.008\,(\text{syst.}), \tag{10}$$

which represents a much less precise measurement than the result of the method described previously.

Both the above results are in agreement with the value

$$\sin^2\theta_W = 0.220 \pm 0.008 \tag{11}$$

compiled from low energy data [13] together with recent results of the CDHS [14] and CCCFRR [15] experiments, after radiative corrections have been applied to these data. Very recent and accurate data from the CDHS [16] and CHARM [17] experiments do not significantly alter the average value of (11).

In the above discussion we have implicitly assumed the ϱ parameter, defined as [18]

$$\varrho = M_W^2/(M_Z^2\cos^2\theta_W) \tag{12}$$

to be $\varrho = 1$, which follows directly from the definition of $\sin^2\theta_W$ given by Eq. (6). However, by combining Eqs. (7) and (12) we obtain

$$\varrho = M_W^2/[M_Z^2(1-B^2/M_W^2)], \tag{13}$$

where $B^2 = A^2/(1-\Delta r)$. In our data this is the only measurable quantity which is sensitive to the Higgs sector (more precisely, it depends on the isospin structure of the Higgs fields, but only very weakly on their masses). From Eq. (13) we obtain

$$\varrho = 0.996 \pm 0.033\,(\text{stat.}) \pm 0.009\,(\text{syst.}), \tag{14}$$

in good agreement with the value $\varrho = 1.02 \pm 0.02$ from low energy data (see the compilations of [28] and [36]), and with the minimal Standard Model.

Finally, we evaluate the sensitivity of our measurements to the radiative corrections expressed in terms of the quantity Δr. Using, only our measurements, and eliminating $\sin^2\theta_W$ from Eqs (7) and (7'), we obtain

$$\Delta r = 0.08 \pm 0.10\,(\text{stat.}) \pm 0.03\,(\text{syst.}). \tag{15}$$

If, on the other hand, we use the average value of $\sin^2\theta_W$ from low energy data (see Eq. (11)), and combine the values of Δr obtained from Eqs (7) and (7'), we obtain [20]

$$\Delta r = 0.05 \pm 0.03\,(\text{stat.}) \pm 0.03\,(\text{syst.}). \tag{16}$$

Within the present statistical and systematic errors, we cannot demonstrate the existence of radiative corrections in the Standard Model, even if we include the results of low energy experiments. This conclusion is summarised in Fig. 10, which shows the 68% confidence

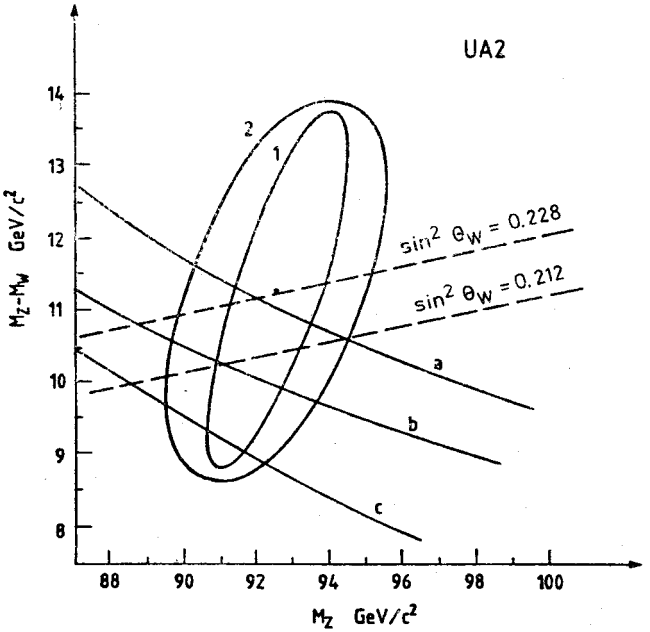

Fig. 10. The UA2 68% confidence contours in the $M_Z - M_W$ vs M_Z plot, (1) taking into account the statistical error only, (2) with statistical and systematic errors added in quadrature. Curve *a* is the Standard Model prediction for $\varrho = 1$ with radiative corrections. Curve *b* is the same prediction without radiative corrections. The band defined by curves *a* and *c* corresponds to the region allowed by the low energy result [10, 9], $\varrho = 1.02 \pm 0.02$. The curves corresponding to two different values of $\sin^2\theta_W$ define the region allowed by the world average of low energy results [13–15], $\sin^2\theta_W = 0.220 \pm 0.008$

level contours in the plot of $M_Z - M_W$ versus M_Z from our measurements, compared to the Standard Model predictions ($\varrho = 1$) with and without radiative corrections. Also shown in Fig. 10 are the ranges of $\sin^2\theta_W$ and ϱ allowed by the low energy measurements.

8. *Conclusions*

Data collected at $\sqrt{s} = 630$ GeV confirm previously published UA2 results at $\sqrt{s} = 546$ GeV. The features of inclusive jet production are well described by QCD calculations. Concerning the Intermediate Vector Bosons, the production cross sections, the values of M_W, M_Z and Γ_Z, and the forward-backward asymmetry in W decays, all agree with the predictions of the minimal electroweak model and QCD. In conclusion all measurements on jet and electron production are in agreement with the standard SU(3) ⊗ SU(2) ⊗ U(1) model of the strong and electroweak interactions.

REFERENCES

[1] UA2, P. Bagnaia et al., *Phys. Lett.* **138B**, 430 (1984); UA2, P. Bagnaia et al., *Phys. Lett.* **144B**, 283 (1984); UA2, P. Bagnaia et al., *Phys. Lett.* **144B**, 291 (1984); UA2, P. Bagnaia et al., *Z. Phys.* **C20**, 117 (1983).

[2] UA2, P. Bagnaia et al., *Phys. Lett.* **139B**, 105 (1984); UA2, M. Banner et al., *Phys. Lett.* **122B**, 476 (1933); UA2, P. Bagnaia et al., *Phys. Lett.* **129B**, 130 (1983); UA2, P. Bagnaia et al., *Z. Phys.* **C24**, 1 (1984).
[3] B. Mansoulié: The UA2 Apparatus at the CERN $\bar{p}p$ Collider, Proc. of the 3rd Moriond Workshop on $\bar{p}p$ Physics (1983), p. 609 (éditions Frontières); M. Dialinas et al., The vertex detector of the UA2 experiment, LAL-RT/83/14 (1983); A. Beer et al., *Nucl. Instrum. Methods* **224**, 360 (1984); C. Conta et al., *Nucl. Instrum. Methods* **224**, 65 (1984); K. Borer et al., *Nucl. Instrum. Methods* **227**, 29 (1984).
[4] E. Eichten et al., *Rev. Mod. Phys.* **56**, 579 (1984).
[5] E. Eichten et al., *Phys. Rev. Lett.* **50**, 811 (1983).
[6] M. Glück et al., *Z. Phys.* **C13**, 119 (1982).
[7] G. Altarelli, R. K. Ellis, M. Greco, G. Martinelli, *Nucl. Phys.* **B246**, 12 (1984); G. Altarelli, R. K. Ellis, G. Martinelli, *Z. Phys.* **C27**, 329 (1984).
[8] M. Kobayashi, K. Maskawa, *Prog. Theor. Phys.* **49**, 652 (1973).
[9] A. Sirlin, *Phys. Rev.* **D22**, 971 (1980); W. J. Marciano, *Phys. Rev.* **D20**, 274 (1979); M. Veltman, *Phys. Lett.* **91B**, 95 (1980); F. Antonelli et al., *Phys. Lett.* **91B**, 90 (1980).
[10] W. J. Marciano, A. Sirlin, *Phys. Rev.* **D29**, 945 (1984).
[11] E. R. Williams, P. T. Olsen, *Phys. Rev. Lett.* **42**, 1575 (1979); G. Bardin et al., *Phys. Lett.* **137B**, 135 (1984); Particle Data Group, *Rev. Mod. Phys.* **56**, 51 (1984).
[12] M. Veltman, *Nucl. Phys.* **B123**, 89 (1977); Z. Hioki, *Nucl. Phys.* **B229**, 284 (1983); B. Lynn, M. Peskin, R. Stuart, SLAC-PUB-3725, July 1985.
[13] W. J. Marciano, A. Sirlin, *Nucl. Phys.* **B189**, 442 (1981); For a more recent review see J. Panman, CERN-EP/85-35 (1985).
[14] H. Abramowicz et al., *Z. Phys.* **C28**, 51 (1985).
[15] P. G. Reutens et al., *Phys. Lett.* **152B**, 404 (1985).
[16] C. Guyot, these proceedings.
[17] F. Bergsma et al., A Precision Measurement of the Ratio of Neutrino-induced Neutral-current and Charged-current Total Cross-sections, CERN-EP/85/113 (1985).
[18] D. Ross, M. Veltman, *Nucl. Phys.* **B95**, 135 (1975); P. Q. Hung, J. J. Sakurai, *Nucl. Phys.* **B143**, 81 (1978).
[19] J. Kim et al., *Rev. Mod. Phys.* **53**, 211 (1980); For more recent reviews see: P. Langacker, Proc. XXII Int. Conf. on High-Energy Physics, Leipzig 1984, pp. 215–238; A. Pullia, *Fifty Years of Weak Interaction Physics*, 1984, pp. 333–415.
[20] The average value of low energy $\sin^2\theta_W$ has been found assuming "standard" radiative corrections (for example $m_t \ll M_W$). If the radiative corrections are non-standard there is another contribution to Δr due to the change in $\sin^2\theta_W$. This contribution is now small compared to the current statistical errors: W. J. Marciano, A. Sirlin, *Phys. Rev.* **D22**, 2695 (1980).
[21] S. D. Ellis, R. Kleiss, W. J. Stirling, *Phys. Lett.* **154B**, 435 (1985).